ARTICLE

Chemical Empiricism 2.0 at Age of Big Data: Large-scale Prediction of Reaction Pathways Based on Bond Dissociation Energies

Shi-lu Chen*

Key Laboratory of Cluster Science of Ministry of Education, School of Chemistry, Beijing Institute of Technology, Beijing 100081, China

A programmable algorithm using bond dissociation energies has been proposed for the prediction of reaction pathways. It has been successfully applied to a gas-phase reaction of F_2+CH_3Cl, with the accurate revelation of the most favorable product CF_4 and its corresponding reaction pathway. This acts as an inspiring example of chemical empiricism 2.0, and may open the door for the large-scale prediction of reaction pathways at the age of big data.

Key words: Big data, Bond dissociation energy, Reaction pathway, Prediction

I. INTRODUCTION

In the past centuries, a large number of chemical empirical methods have been created and worked in various aspects of chemistry [1]. They have been and are fruitful for the development of science, even if advancements in modern physics, in particular the development of quantum mechanics (QM), have made it possible to *ab initio* explore diverse chemical issues. In this age of chemical empiricism 1.0, it was often found that some non-well-theorized empirical formulas, which might be simply derived from limited evidences, work very well in the fields where QM could not perfectly account for yet. Nowadays, with an uncountable number of chemical data accumulated from experiments and theories, coupled with the nearly exponential growth of computer power, we are welcoming chemical empiricism 2.0 at a new age of big data, a combination of chemical intuition and abundant QM data (*i.e.*, QM simulations). Using a simple but well-defined algorithm that originates from chemical intuition, one can today routinely handle systems containing countless QM-derived data, which may open the door for the large-scale prediction in various chemical fields based on big data of QM simulations. On the other hand, the successful prediction based on big data may optimize chemists' intuition, facilitating the development of new chemical methods.

One of the fields that chemical empiricism 2.0 may have positive impact on is the prediction of reaction pathways, which is usually believed to be of high difficulty and only handleable by high-level QM methods. In this work, a simple and programmable algorithm is

———————

*Author to whom correspondence should be addressed. E-mail: shlchen@bit.edu.cn

proposed for the large-scale prediction of reaction pathways, based on bond dissociation energies (BDEs), a type of simple QM-derived data. The BDEs used in the prediction procedure can be easily obtained by automatic calculations using high-level QM methods, such as the density functional theory (DFT). The specific reaction under consideration is a gas-phase reaction of F_2+CH_3Cl. The algorithm proposed here has been successfully applied to this reaction, in particular accurately revealing the most favorable product (CF_4) and its reaction pathway. This demonstrates that the algorithm is capable of predicting pathways of the reactions where radicals are dominant intermediates, and thus acts as a successful example of chemical empiricism 2.0 at the age of big data.

II. PREDICTION ALGORITHM

An algorithm for the prediction of reaction pathways, which is programable, is schematically presented in Scheme 1.

All reactants are first split into fragments by exhaustively enumerative homolysis of every chemical bond [2]. The resultant fragments are referred to as first-order fragments (FOFs). Every molecule/fragment emerging in the prediction algorithm is marked by a unique numerical label. The bond dissociation energy (BDE) corresponding to each homolysis is automatically calculated by high-level QM methods (described later) and recorded with a unique label. Secondly, enumerative coupling among FOFs are performed, leading to a series of products (referred to as first-order products, FOPs). The repeating couplings and the ones back to reactants are omitted. The bond formation energy (BFE) for each coupling is equal to the minus of corresponding BDE and is calculated by the same quantum chemical method. The reaction pathway for the formation of
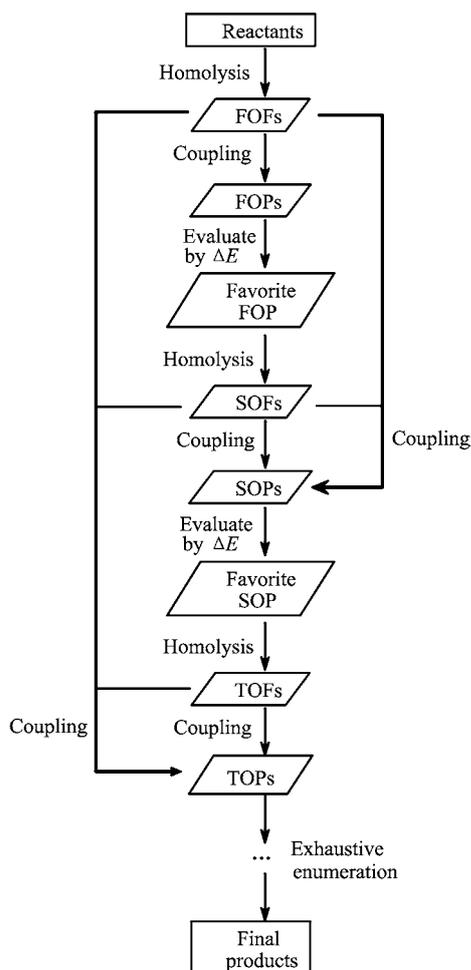
Scheme 1 Schematic algorithm for the prediction of reaction pathways. FOF: first-order fragment. FOP: first-order product. SOF: second-order fragment. SOP: second-order product. TOF: three-order fragment. TOP: three-order product. E: reaction energy.

each FOP is defined as the corresponding FOF formation via the homolysis of reactants, followed by the coupling of the FOFs. The reaction energy (ΔE) is calculated by the sum of BDEs and BFEs along the reaction pathway. It should be noted that all reaction pathways as well as their ΔE should be regulated to have the same amount of reactants (at least with one reactant as the reference). Then, all reaction pathways are assessed by comparing their ΔE with several criteria. (i) The pathway with the smallest ΔE is favorite. (ii) If several pathways are calculated to have significantly negative ΔE, all of them are favorable even though their ΔE are quite different. (iii) The one with smaller BDE of FOFs is preferential when ΔE are close or significantly negative. (iv) When all ΔE of FOPs are positive, in principle the selected pathway should not have too big ΔE; otherwise, all reaction pathways should be ruled out. (v) In general only one pathway excels others; if several paths are undistinguishable by the former four

rules, all of them are elected.

The subsequent reactions of the favorite FOP follow the same pattern as the case of reactants, *i.e.*, the breaking of FOP to second-order fragments (SOFs) by exhaustively enumerative homolysis of every chemical bond, followed by the coupling of resultant SOFs with all FOFs as well as SOFs, resulting in second-order products (SOPs). The formation of SOPs is evaluated with their corresponding ΔE via the same rules for FOPs (described earlier). The same treatments are then applied to the favorite SOP and the following products until all possible fragments and products derived via the five criteria described above are exhaustively enumerated.

It is worth noting that only thermodynamics is considered in this algorithm. Although it is impossible to estimate reaction rate, the energy barrier in each reaction pathway is to a certain extent dependent on the ΔE, since the raise/drop of product parabola may result in the same shift of the intersection with reactant parabola, thus leading to the increase/decrease of barrier height. This speculation may be quite close to the truth in a displacement reaction where reactant states are the same in many tested pathways, for example, in the specific case of F_2+CH_3Cl studied here.

All quantum chemical calculations presented in this work were performed using unrestricted DFT with the hybrid functional B3LYP [3−5] as implemented in Gaussian 09 package [6]. With dispersion included, geometry optimizations were carried out using the 6-311++G(d,p) basis set. Dispersion corrections were considered using the empirical formula by Grimme *et al.* (*i.e.*, DFT-D3) [7−10]. BDEs were calculated by:

$$BDE = E - E_{\text{molecule}} \qquad (1)$$

where E is energy sum of separated fragments, while E_{molecule} is energy of molecule. In the future calculations of BDEs, more effects, such as temperature, pressure, solvent, and so on, may be introduced to more accurately adapt to complicated gas-phase, liquid-phase, and even heterogeneous reactions.

Furthermore, it will be valuable to construct a special database to store the BDEs which are collected from reliable experiments and previous QM calculations. The prediction program can directly read the data when the needed BDEs have already been stored in the database. If the BDEs are unavailable, necessary QM calculations will be preformed and the obtained BDEs will be saved in the database in time. This should greatly speed up the prediction of reaction pathways.

III. RESULTS AND DISCUSSION

Using the prediction algorithm described earlier, the reaction of F_2+CH_3Cl has been analyzed. The formation of first-order products (FOPs) is shown in Fig.1. The calculated BDEs are given in Table I.

TABLE I Bond dissociation energies (BDEs, in kcal/mol) calculated by B3LYP-D3/6-311++G(d,p).

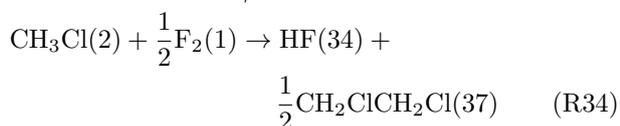| Label	Homolysis reaction	BDE	Label	Homolysis reaction	BDE
1a	$F_2(1) \rightarrow 2F(3)$	31.8	33a	$ClF(33) \rightarrow F(3)+Cl(5)$	52.7
2a	$CH_3Cl(2) \rightarrow CH_3(4)+Cl(5)$	82.0	34a	$HF(34) \rightarrow F(3)+H(7)$	137.8
2b	$CH_3Cl(2) \rightarrow CH_2Cl(6)+H(7)$	105.5	35a	$CH_4(35) \rightarrow CH_3(4)+H(7)$	110.8
8a	$CH_3F(8) \rightarrow CH_3(4)+F(3)$	110.7	36a	$HCl(36) \rightarrow H(7)+Cl(5)$	103.5
8b	$CH_3F(8) \rightarrow CH_2F(11)+H(7)$	106.5	37a	$(CH_2Cl)_2(37) \rightarrow 2CH_2Cl(6)$	88.9
9a	$Cl_2(9) \rightarrow 2Cl(5)$	47.6	38a	$H_2(38) \rightarrow 2H(7)$	109.9
10a	$CH_2ClF(10) \rightarrow CH_2F(11)+Cl(5)$	81.4	39a	$CH_3CH_2F(39) \rightarrow CH_2F(11)+CH_3(4)$	94.4
10b	$CH_2ClF(10) \rightarrow CH_2Cl(6)+F(3)$	108.9	40a	$CH_2FCH_2Cl(40) \rightarrow CH_2F(11)+CH_2Cl(6)$	90.7
13a	$CH_2F_2(13) \rightarrow CH_2F(11)+F(3)$	117.1	41a	$CH_2FCH_2F(41) \rightarrow 2CH_2F(11)$	92.1
13b	$CH_2F_2(13) \rightarrow CHF(14)+H(7)$	106.4	42a	$CH_3CHF_2(42) \rightarrow CHF_2(14)+CH_3(4)$	97.5
15a	$CH_2Cl_2(15) \rightarrow CH_2Cl(6)+Cl(5)$	75.7	43a	$CH_2ClCHF_2(43) \rightarrow CHF_2(14)+CH_2Cl(6)$	90.9
17a	$CHClF_2(17) \rightarrow CHF_2(14)+Cl(5)$	80.6	44a	$CH_2FCHF_2(44) \rightarrow CHF_2(14)+CH_2F(11)$	92.9
21a	$CHF_3(21) \rightarrow CHF_2(14)+F(3)$	121.9	45a	$CHF_2CHF_2(45) \rightarrow 2CHF_2(14)$	91.0
21b	$CHF_3(21) \rightarrow CF_3(22)+H(7)$	111.1	46a	$CH_3CF_3(46) \rightarrow CF_3(22)+CH_3(4)$	102.6
25a	$CClF_3(25) \rightarrow CF_3(22)+Cl(5)$	79.8	47a	$CH_2ClCF_3(47) \rightarrow CF_3(22)+CH_2Cl(6)$	93.2
28a	$CF_4(28) \rightarrow CF_3(22)+F(3)$	122.7	48a	$CH_2FCF_3(48) \rightarrow CF_3(22)+CH_2F(11)$	95.6
30a	$CH_3CH_3(30) \rightarrow 2CH_3(4)$	92.7	49a	$CHF_2CF_3(49) \rightarrow CF_3(22)+CHF_2(14)$	91.4
32a	$CH_3CH_2Cl(32) \rightarrow CH_3(4)+CH_2Cl(6)$	91.8	50a	$CF_3CF_3(50) \rightarrow 2CF_3(22)$	91.3

The F_2 reactant (labeled by 1) was broken to two F atoms (3) with a BDE of 31.8 kcal/mol (named by 1a), while $CH_3Cl(2)$ was separated by two ways, *i.e.* into $CH_3(4)+Cl(5)$ with a BDE of 2a=82.0 kcal/mol and into $CH_2Cl(6)+H(7)$ with a BDE of 2b=105.5 kcal/mol. The coupling between first-order fragments (3, 4, 5, 6, and 7) were then performed to produce various FOPs with the related reaction energies (ΔE) calculated. Three reactions were found to have significantly negative ΔE. They are

$$CH_3Cl(2) + \frac{1}{2}F_2(1) \rightarrow CH_3F(8) + \frac{1}{2}Cl_2(9) \quad (R8)$$

$$\Delta E_8 = 2a - 8a + \frac{1}{2}1a - \frac{1}{2}9a$$
$$= -36.6 \text{ kcal/mol}$$

$$CH_3Cl(2) + \frac{1}{2}F_2(1) \rightarrow CH_2ClF(10) + \frac{1}{2}H_2(38) \quad (R10)$$

$$\Delta E_{10} = 2b - 10b + \frac{1}{2}1a - \frac{1}{2}38a$$
$$= -42.4 \text{ kcal/mol}$$

$$CH_3Cl(2) + \frac{1}{2}F_2(1) \rightarrow HF(34) +$$
$$\frac{1}{2}CH_2ClCH_2Cl(37) \quad (R34)$$

$$\Delta E_{34} = 2b - 34a + \frac{1}{2}1a - \frac{1}{2}37a$$
$$= -60.8 \text{ kcal/mol}$$

These three reactions were thus predicted to be favorable. In real system, the dissociation of F_2 to F atoms should be an initial step since its BDE (1a=31.8 kcal/mol) is considerably smaller than

those in the CH_3Cl homolysis (2a=82.0 kcal/mol and 2b=105.5 kcal/mol). The resultant F atom may attack CH_3Cl through three ways. The attack of F on the carbon of CH_3Cl should initiate a S_N2-type displacement to produce CH_3F+Cl or CH_2ClF+H, while the attack on the hydrogen of CH_3Cl leads to $HF+CH_2Cl$. Subsequently, the homologous coupling of the resulting radicals (Cl, H, and CH_2Cl) may take place to form another products in these three reactions (Cl_2, H_2, and CH_2ClCH_2Cl). With this, it can be concluded that the present algorithm gives a reasonable prediction for the formation of FOPs in this particular case of F_2+CH_3Cl.

A further analysis on the formation of FOFs indicates that reaction (R8) costs the smallest energy in the step of FOF formation, compared with reactions (R10) and (R34). The cost energies are 97.9 kcal/mol ($2a+\frac{1}{2}1a$), 121.4 kcal/mol ($2b+\frac{1}{2}1a$), and 121.4 kcal/mol ($2b+\frac{1}{2}1a$) for reactions (R8), (R10), and (R34), respectively. This implies that reaction (R8) may be the favorite one although its ΔE is the highest among these three reactions. This predicted result is consistent with chemical common sense. The corresponding reaction pathway for reaction (R8) is formulated as

$$CH_3Cl(2) \xrightarrow[+2a]{} CH_3(4) + Cl(5)$$
$$\xrightarrow[-8a]{+F(3)} CH_3F(8) + Cl(5)$$
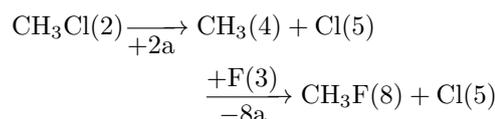
The FOPs of the favorite reaction (R8) (*i.e.*, CH_3F and Cl_2) were included in the following formation of
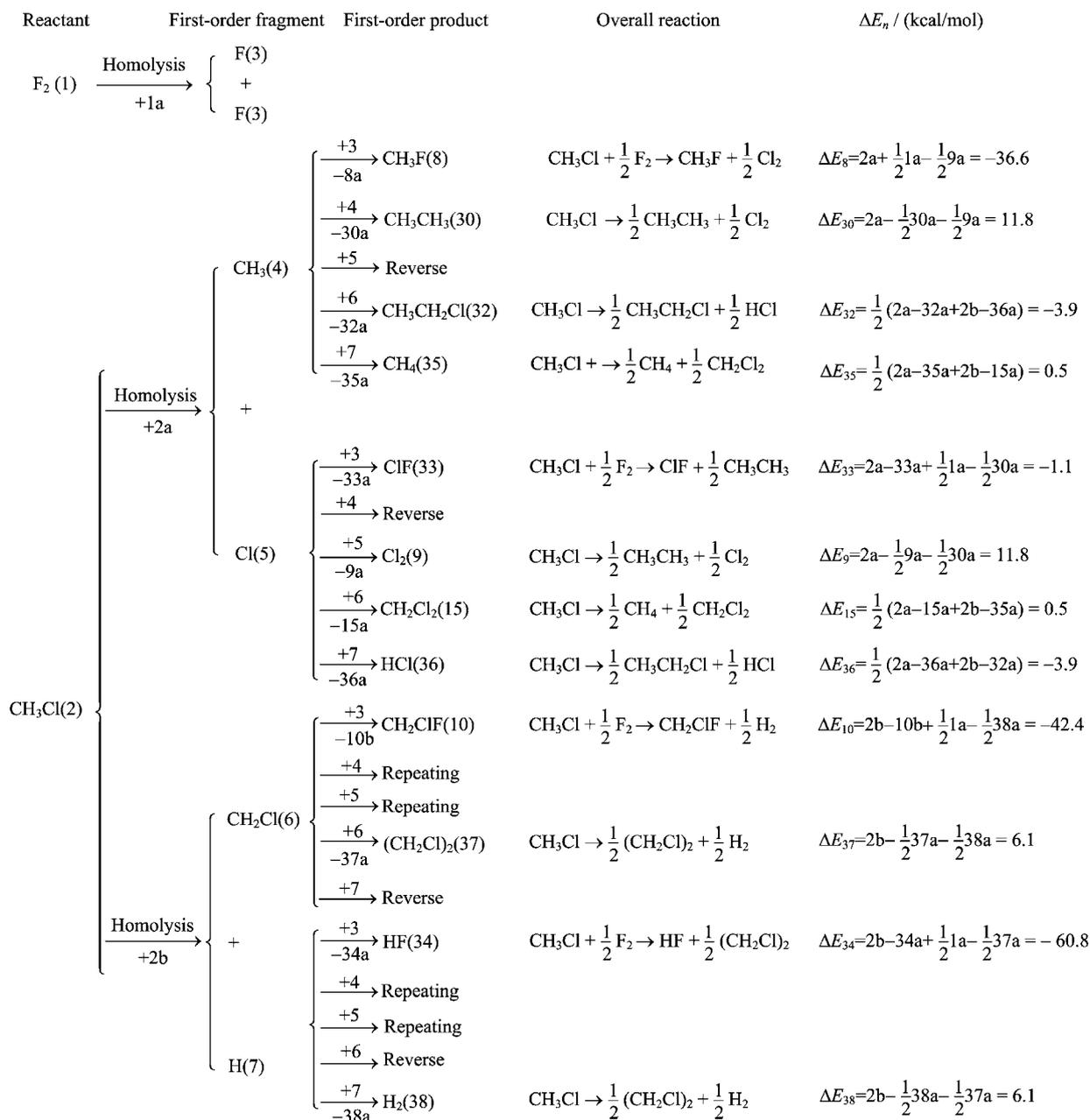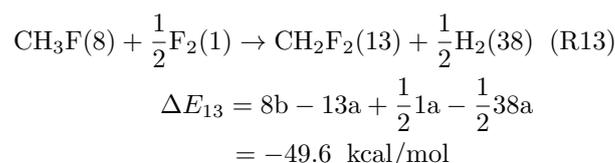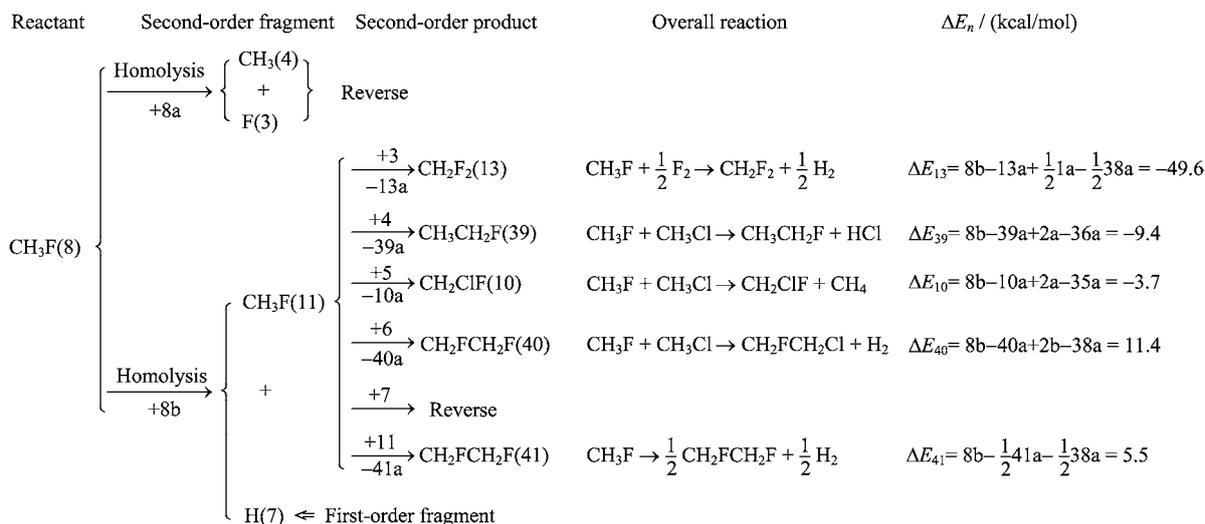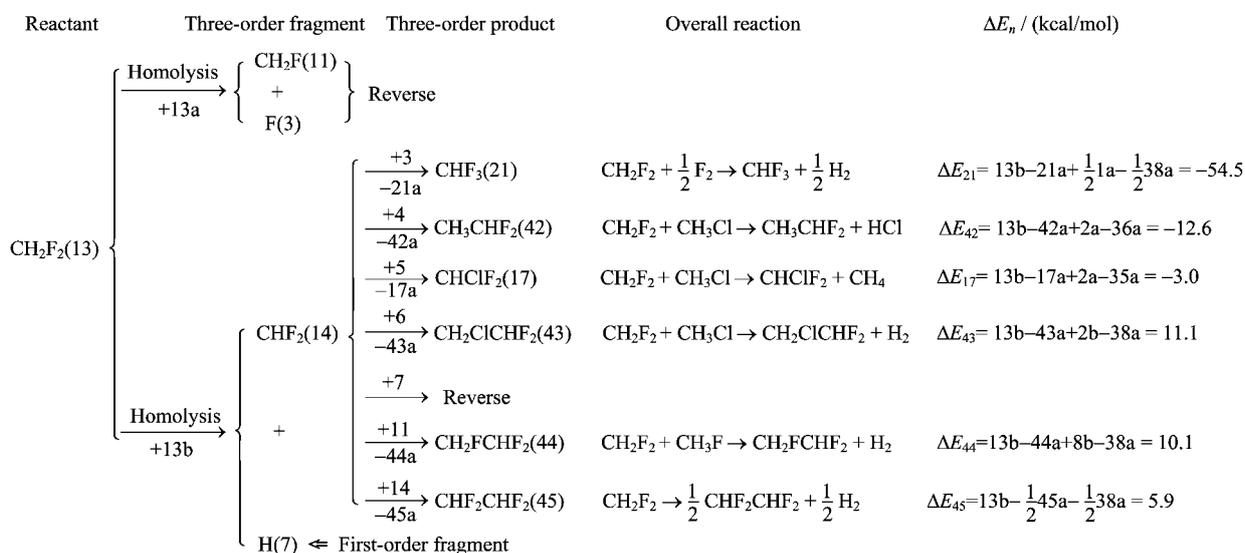
FIG. 1 Reaction pathways for the formation of first-order products. The labels below arrows indicate bond dissociation energies.

second-order fragments and products. The breaking of Cl_2 can be further omitted since it is actually a reverse process of the Cl_2 formation. Therefore, only $CH_3F(8)$ was considered as the reacting FOP in the subsequent calculations of the formation of SOPs (see Fig.2). $CH_3F(8)$ was dissociated to $CH_2F(11)+H(7)$ with a BDE of 8b=106.5 kcal/mol or to $CH_3(4)+F(3)$ with a BDE of 8a=110.7 kcal/mol. The latter can be omitted because it is a reverse reaction back to the first-order product of $CH_3F(8)$. In addition, considering that the fragment of $H(7)$ is not a new species but a FOF, only the SOF of $CH_2F(11)$ was involved in the next cou-

pling of fragments. The coupling of $CH_2F(11)$ were carried out with every FOF and then SOF. The reverse and repeating processes were excluded. It has been found that, with $CH_3F(8)$ as the reactant state, the favorite reaction for the SOP formation is

$$CH_3F(8) + \frac{1}{2}F_2(1) \rightarrow CH_2F_2(13) + \frac{1}{2}H_2(38) \quad (R13)$$

$$\Delta E_{13} = 8b - 13a + \frac{1}{2}1a - \frac{1}{2}38a$$

$$= -49.6 \text{ kcal/mol}$$

Its ΔE is much lower than those of other reactions, at

Reactant	Second-order fragment	Second-order product	Overall reaction	ΔE_n / (kcal/mol)

$$CH_3F(8) \begin{cases} \xrightarrow[+8a]{Homolysis} \left\{ \begin{array}{c} CH_3(4) \\ + \\ F(3) \end{array} \right\} \; Reverse \\ \\ \xrightarrow[+8b]{Homolysis} \end{cases}$$

CH$_3$F(11)
+

$\xrightarrow[-13a]{+3}$ CH$_2$F$_2$(13)   CH$_3$F + $\frac{1}{2}$F$_2$ → CH$_2$F$_2$ + $\frac{1}{2}$H$_2$ ΔE_{13}= 8b−13a+$\frac{1}{2}$1a−$\frac{1}{2}$38a = −49.6

$\xrightarrow[-39a]{+4}$ CH$_3$CH$_2$F(39)   CH$_3$F + CH$_3$Cl → CH$_3$CH$_2$F + HCl ΔE_{39}= 8b−39a+2a−36a = −9.4

$\xrightarrow[-10a]{+5}$ CH$_2$ClF(10)   CH$_3$F + CH$_3$Cl → CH$_2$ClF + CH$_4$ ΔE_{10}= 8b−10a+2a−35a = −3.7

$\xrightarrow[-40a]{+6}$ CH$_2$FCH$_2$F(40)   CH$_3$F + CH$_3$Cl → CH$_2$FCH$_2$Cl + H$_2$ ΔE_{40}= 8b−40a+2b−38a = 11.4

$\xrightarrow{+7}$ Reverse

$\xrightarrow[-41a]{+11}$ CH$_2$FCH$_2$F(41)   CH$_3$F → $\frac{1}{2}$CH$_2$FCH$_2$F + $\frac{1}{2}$H$_2$ ΔE_{41}= 8b−$\frac{1}{2}$41a−$\frac{1}{2}$38a = 5.5
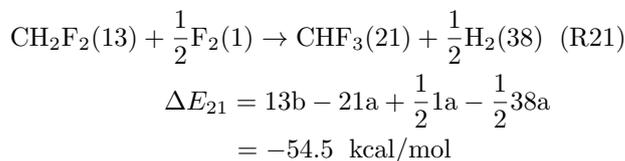
H(7) ⇐ First-order fragment

FIG. 2 Reaction pathways for the formation of second-order products from the favorite first-order product (CH$_3$F).

Reactant	Three-order fragment	Three-order product	Overall reaction	ΔE_n / (kcal/mol)

$$CH_2F_2(13) \begin{cases} \xrightarrow[+13a]{Homolysis} \left\{ \begin{array}{c} CH_2F(11) \\ + \\ F(3) \end{array} \right\} \; Reverse \\ \\ \xrightarrow[+13b]{Homolysis} \end{cases}$$

CHF$_2$(14)
+

$\xrightarrow[-21a]{+3}$ CHF$_3$(21)   CH$_2$F$_2$ + $\frac{1}{2}$F$_2$ → CHF$_3$ + $\frac{1}{2}$H$_2$ ΔE_{21}= 13b−21a+$\frac{1}{2}$1a−$\frac{1}{2}$38a = −54.5

$\xrightarrow[-42a]{+4}$ CH$_3$CHF$_2$(42)   CH$_2$F$_2$ + CH$_3$Cl → CH$_3$CHF$_2$ + HCl ΔE_{42}= 13b−42a+2a−36a = −12.6

$\xrightarrow[-17a]{+5}$ CHClF$_2$(17)   CH$_2$F$_2$ + CH$_3$Cl → CHClF$_2$ + CH$_4$ ΔE_{17}= 13b−17a+2a−35a = −3.0

$\xrightarrow[-43a]{+6}$ CH$_2$ClCHF$_2$(43)   CH$_2$F$_2$ + CH$_3$Cl → CH$_2$ClCHF$_2$ + H$_2$ ΔE_{43}= 13b−43a+2b−38a = 11.1

$\xrightarrow{+7}$ Reverse

$\xrightarrow[-44a]{+11}$ CH$_2$FCHF$_2$(44)   CH$_2$F$_2$ + CH$_3$F → CH$_2$FCHF$_2$ + H$_2$ ΔE_{44}=13b−44a+8b−38a = 10.1

$\xrightarrow[-45a]{+14}$ CHF$_2$CHF$_2$(45)   CH$_2$F$_2$ → $\frac{1}{2}$CHF$_2$CHF$_2$ + $\frac{1}{2}$H$_2$ ΔE_{45}=13b−$\frac{1}{2}$45a−$\frac{1}{2}$38a = 5.9

H(7) ⇐ First-order fragment

FIG. 3 Reaction pathways for the formation of three-order products from the favorite second-order product (CH$_2$F$_2$).

least by 40.2 kcal/mol. The corresponding pathway for reaction (R13) is written as

$$CH_3F(8) \xrightarrow[+8b]{} CH_2F(11) + H(7)$$
$$\xrightarrow[-13a]{+F(3)} CH_2F_2(13) + H(7)$$
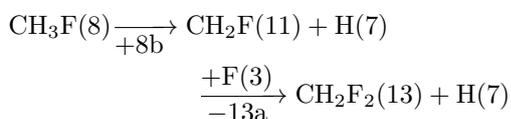
Since H$_2$(38) or H(7) is again a first-order product or fragment, only the second-order product of CH$_2$F$_2$(13) was chosen as the reactant state for the formation of three-order products (TOPs) (see Fig.3). Following the same pattern as the dissociation of CH$_3$F(8), the separation of CH$_2$F$_2$(13) to CH$_2$F(11)+F(3), a reverse process, was skipped, while the one to CHF$_2$(14)+H(7) was kept. Again, only the three-order fragment (TOF) of CHF$_2$(14) was selected for the subsequent coupling

as H(7) is a first-order fragment. The combination of CHF$_2$(14) with every FOF, SOF, and then TOF reveals the preferred reaction for the formation of TOPs,

$$CH_2F_2(13) + \frac{1}{2}F_2(1) \to CHF_3(21) + \frac{1}{2}H_2(38) \quad (R21)$$
$$\Delta E_{21} = 13b - 21a + \frac{1}{2}1a - \frac{1}{2}38a$$
$$= -54.5 \text{ kcal/mol}$$

The corresponding pathway from CH$_2$F$_2$(13) is formulated as

$$CH_2F_2(13) \xrightarrow[-13b]{} CHF_2(14) + H(7)$$
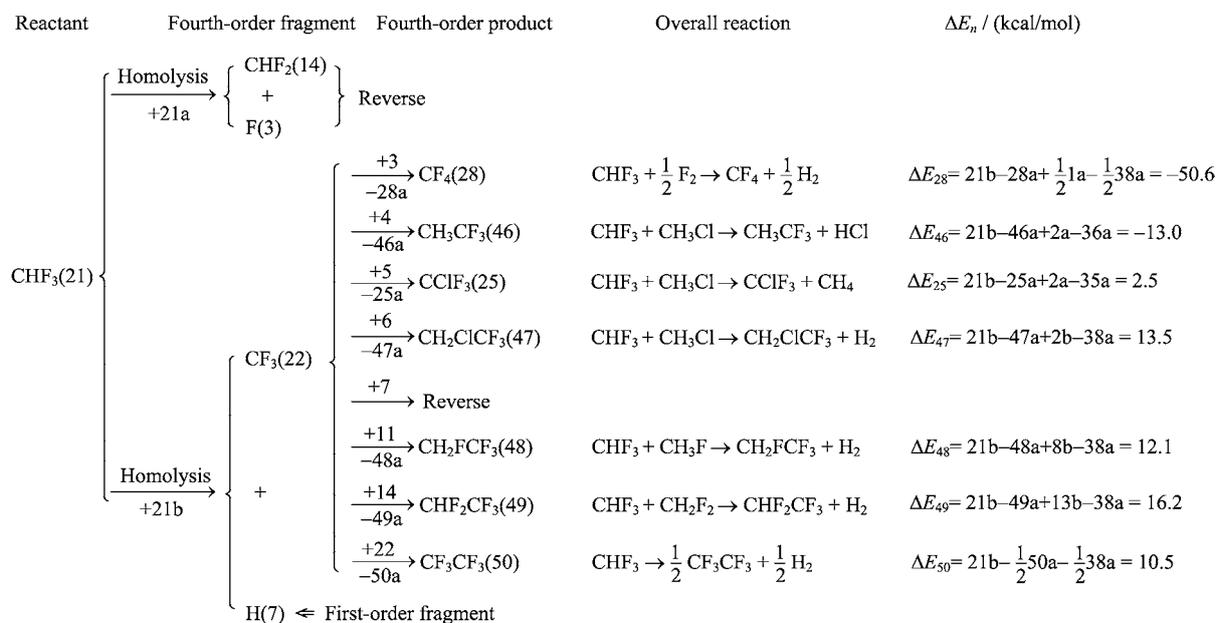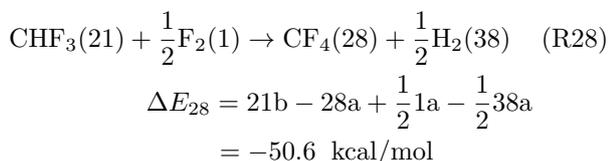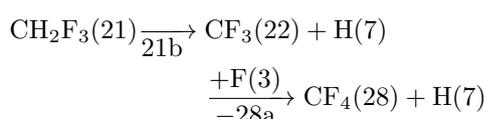$$\xrightarrow[-21a]{+F(3)} CHF_3(21) + H(7)$$
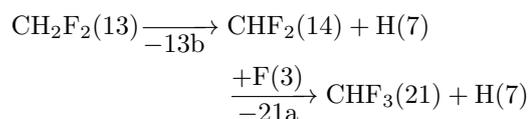
FIG. 4 Reaction pathways for the formation of fourth-order products from the favorite three-order product (CHF_3).

The resultant three-order product of $CHF_3(21)$ then worked as the reactant state for the formation of fourth-order products (OOPs) (Fig.4). $CHF_3(21)$ was decomposed to $CHF_2(14)+F(3)$ or $CF_3(22)+H(7)$. Again, only the fourth-order fragment (OOF) of $CF_3(22)$ was used in the next step of coupling with FOFs, SOFs, TOFs, and OOFs. The favorite reaction for the formation of OOPs was found to be

$$CHF_3(21) + \frac{1}{2}F_2(1) \rightarrow CF_4(28) + \frac{1}{2}H_2(38) \quad (R28)$$

$$\Delta E_{28} = 21b - 28a + \frac{1}{2}1a - \frac{1}{2}38a$$

$$= -50.6 \text{ kcal/mol}$$

Its related pathway from $CHF_3(21)$ is:

$$CH_2F_3(21) \xrightarrow{21b} CF_3(22) + H(7)$$

$$\xrightarrow[-28a]{+F(3)} CF_4(28) + H(7)$$

It can be seen that, after four-order treatments, the most favored product in overall reaction of F_2+CH_3Cl was predicted to be $CF_4(28)$, a very reasonable result that is consistent with the chemical fact. This indicates that the present algorithm is competent for the prediction of reaction pathways of the reactions where gas-phase radicals may be dominant intermediates. The complete pathway for the formation of the favorite $CF_4(28)$ is summarized in Fig.5.

The overall reaction for the CF_4 formation is devised as

$$CH_3Cl(2) + 4F(3) \rightarrow CF_4(28) + 3H(7) + Cl(5)$$

$$\Delta E = 2a - 8a + 8b - 13a + 13b - 21a + 21b - 28a = -66.4 \text{ kcal/mol}$$
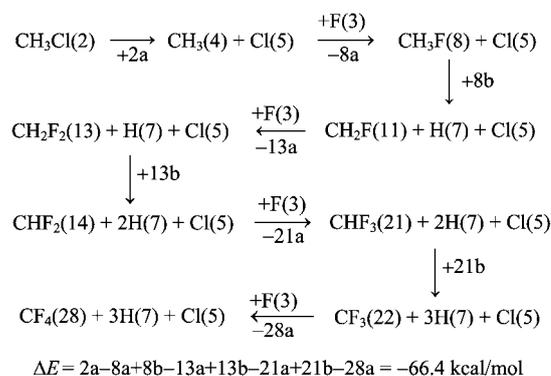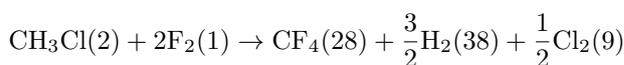
FIG. 5 The complete pathway for the formation of the favorite $CF_4(28)$.

If homologous coupling between the radicals of F, H, and Cl are performed, the favorite overall reaction can be written as

$$CH_3Cl(2) + 2F_2(1) \rightarrow CF_4(28) + \frac{3}{2}H_2(38) + \frac{1}{2}Cl_2(9)$$

With three BDEs ($2(1a)$, $(-3/2)38a$, and $(-1/2)9a$) added, the corresponding overall reaction energy (ΔE) for the CF_4 formation is further calculated to be -191.4 kcal/mol, indicating that it is an energetically reachable reaction.

IV. CONCLUSION

In this work, a programmable algorithm for the prediction of reaction pathways has been proposed, based on the big data of bond dissociation energy (BDE).

Combined with the DFT calculations of BDEs, it succeeds in the prediction of the reaction of F_2+CH_3Cl, successfully revealing the most favorable product (CF_4) and its corresponding reaction pathway. This demonstrates that the algorithm is competent for the treatment of gas-phase reactions where radical intermediates dominate. The exploration here provides an inspiring example of chemical empiricism 2.0, and may open the door for the large-scale digital prediction of reaction pathways at the age of big data. With more techniques introduced, this algorithm may be available for more complicated reactions, such as the ones involving unsaturated bonds and chemical addition steps. If catalysts are regarded as a kind of reactant states, the algorithm may also be developed to be applicable to the catalysis, an exceedingly attractive future.

V. ACKNOWLEDGMENTS

[1] https://en.wikipedia.org/wiki/Empiricism

[2] R. G. A. Bone and H. O. Villar, J. Comput. Chem. **18**, 86 (1997).

[3] A. D. Becke, J. Chem. Phys. **98**, 1372 (1993).

[4] A. D. Becke, J. Chem. Phys. **98**, 5648 (1993).

[5] C. T. Lee, W. T. Yang, and R. G. Parr, Phys. Rev. B **37**, 785 (1988).

[6] M. J. Frisch, G. W. Trucks, H. B. Schlegel, G. E. Scuseria, M. A. Robb, J. R. Cheeseman, G. Scalmani, V. Barone, B. Mennucci, G. A. Petersson, H. Nakatsuji, M. Caricato, X. Li, H. P. Hratchian, A. F. Izmaylov, J. Bloino, G. Zheng, J. L. Sonnenberg, M. Hada, M. Ehara, K. Toyota, R. Fukuda, J. Hasegawa, M. Ishida, T. Nakajima, Y. Honda, O. Kitao, H. Nakai, T. Vreven, J. A. Jr. Montgomery, J. E. Peralta, F. Ogliaro, M. Bearpark, J. J. Heyd, E. Brothers, K. N. Kudin, V. N. Staroverov, R. Kobayashi, J. Normand, K. Raghavachari, A. Rendell, J. C. Burant, S. S. Iyengar, J. Tomasi, M. Cossi, N. Rega, J. M. Millam, M. Klene, J. E. Knox, J. B. Cross, V. Bakken, C. Adamo, J. Jaramillo, R. Gomperts, E. Stratmann, O. Yazyev, A. J. Austin, R. Cammi, C. Pomelli, J. W. Ochterski, R. L. Martin, K. Morokuma, V. G. Zakrzewski, G. A. Voth, P. Salvador, J. J. Dannenberg, S. Dapprich, A. D. Daniels, Ö. Farkas, J. B. Foresman, J. V. Ortiz, J. Cioslowski, and D. J. Fox, *Gaussian 09, Revision D.01*, Wallingford CT: Gaussian, Inc., (2009).

[7] S. Grimme, J. Comput. Chem. **25**, 1463 (2004).

[8] S. Grimme, J. Comput. Chem. **27**, 1787 (2006).

[9] S. Grimme, J. Antony, S. Ehrlich, and H. Krieg, J. Chem. Phys. **132**, 154104 (2010).

[10] L. Goerigk and S. Grimme, Phys. Chem. Chem. Phys. **13**, 6670 (2011).